WARSAW UNIVERSITY OF TECHNOLOGY Index 351733
FACULTY OF CIVIL ENGINEERING
COMMITTEE FOR CIVIL AND WATER ENGINEERING
POLISH ACADEMY OF SCIENCES ISSN 1230-2945

DOI: 10.24425/ace.2020.131771
ARCHIVES OF CIVIL ENGINEERING
Vol. LXVI ISSUE 1 2020

RELIABLE CRACK WIDTH PREDICTION IN EN 13084 & CICIND

P. Noakowski, A. Harling

Cracks in concrete are inevitable but fortunately cracking enables the structures to get rid of its bending moment peaks. The reduction is due to the redistribution of the load induced moments and cut of the temperature-imposed moments. However, cracking becomes completely harmless if the crack widths are controlled properly by reinforcement. In this regard a method for crack width prediction is presented in this paper which thanks its reliability is widely accepted in the standards EN 13084, CICIND and DIN 1056.

Keywords: Advanced design of r/c structures, crack width, safety, tightness, durability minimum reinforcement, non-linear analysis

1. BACKGROUND

1.1 Threats by wide separating Cracks, Fig. 1.1, [21]

Most damages in reinforced concrete structures are attributable to wide through cracks which separate the component into individual portions. One of the classical examples for such thread is the depicted chimney windshield impaired by wide vertical cracks separating the windshield into individual strips, which had led to the following abnormal behaviour:

(1) Normal cracks due to enough hoop reinforcement - regular vertical stresses

(2) Separating cracks due to insufficient hoop reinforcement - increased vertical stresses

As the crack width limitation was improper the wind shield was furnished with insufficient hoop reinforcement. This led to formation of wide cracks subdividing the shell into individual nearly free-standing strips, which during a hurricane couldn't withstand excessive vertical compression and bulged out. So the crack width control is not only for aesthetics, durability and tightness but also for the securing of the structural integrity which is needed to retain the basic static system and to prevent loss of the load bearing capacity.

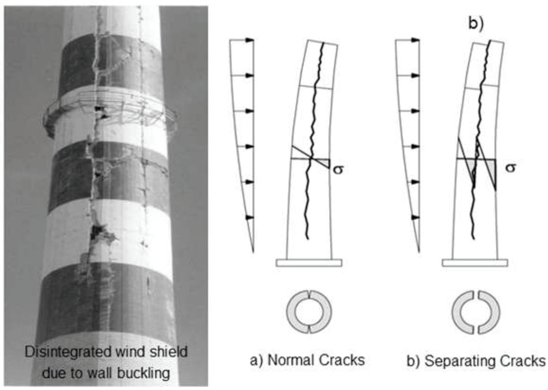

Fig. 1.1: BACKGROUND, Threats by wide separating cracks
Loss of the wind load bearing capacity due to wide separating cracks
a) Normal cracks due to enough hoop reinforcement, Regular vertical stresses
b) Separating cracks due to insufficient hoop reinforcement, Increased vertical stresses

1.2 IMPAIRMENTS BY WIDE CRACKS, Fig 1.2, [21]

Excessive cracks can also cause other improper sorts of the structure behaviour:

(1) Impairment of the visibility of industrial chimneys by depositions of dirt into wide cracks in painting

(2) Destruction of the integrity of chimneys by water intrusion into wide cracks and ice formation

(3) Endangering of the bearing capacity of cooling towers by shell subdivision into free-standing walls

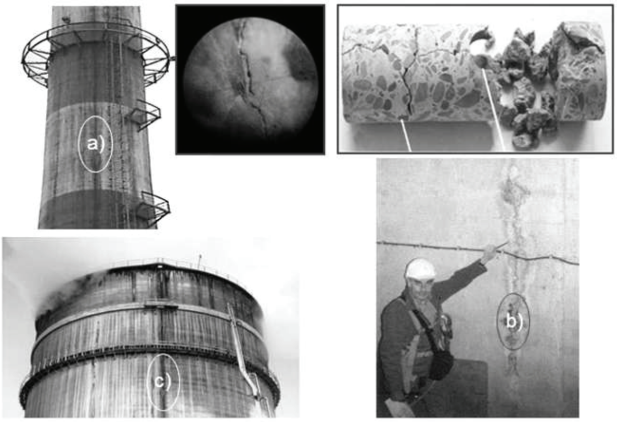

Fig 1.2: BACKGROUND, Impairment by Wide Cracks

a) Impairment of the visibility of industrial chimneys by depositions of dirt into wide cracks in painting

b) Destruction of the integrity of industrial chimneys by water intrusion into wide cracks and ice formation

1.3 ACCEPTANCE OF THE METHOD

To prevent problems with cracks, the Continuous Deformation Theory (CDT) [07,15,16, 22, 28, 31] was developed, whose closeness to reality and simplicity in use have led to its wide acceptance in research [01, 06, 25, 29, 30, 32, 37], relevant standards [02, 03, 04, 05, 12, 18] and dimensioning practice [09, 10, 11, 14, 17, 19, 20, 21, 23, 24, 26, 27, 34, 35]. The CDT is used particularly often in planning and assessment of industrial structures, where extreme actions and stringent requirements are involved. There were also used the publications [01, 08, 33, 36].

Due to all these the crack control method based on the CDT was accepted in the following standards:

- DIN 1056 Commentary on Industrial Chimneys, by Nieser & Engel, 1986 [12]
- CICIND Model Code & Commentaries for Concrete Chimneys, Part A: The Shell, August 2001 [02]
- EN 13084-2: Free-standing Chimneys, Part 2: Concrete Chimneys, January 2007 [03]

This crack prediction method is presented in the paper at hand in term of its Background, Bases, Method, Reliability and Appliance.

2. BASES

2.1 DEFORMATION BEHAVIOR, FIG. 2.1, [7,15,16, 22, 28, 31]

2.1.1 DEFORMATION LAW

To understand the nature of the crack formation, the polygon like deformation laws must be explained by using four cracking ranges:

Range 0: No cracks: Initial high stiffness due to lack of cracks

Range 1: First Crack Formation: Increasing number of individual cracks located far from each other

Range 2: Final Crack Formation: Final number of numerous cracks with overlapping transition areas

Range 3: Steel Yielding: Plasticization of reinforcement at cracks

2.1.2 FIRST CRACK FORMATION

The first cracks occur when the bending moment M, activated mostly by temperature difference reaches its cracking value Mcr. Further increase of ΔT leads only to further cracks without change of Mcr. The individual cracks, located far apart from each other, are having invisible transition lengths of a1 in which the steel bar is displaced against concrete. The entire behavior with increasing temperature difference ΔT is as follows:

Bending moment	M_{cr}	constant
Transition length	a_1	constant
Steel stress	σ_{cr}	constant
Crack width	w	constant
Crack number	n_{cr}	increasing

2.1.3 FINAL CRACK FORMATION

The final crack occurs when the bending moment M activated by external loads excels the cracking value Mcr. This produces the final stable number of cracks whose visible spacing overlaps and varies between a1/2 and a1. The crack propagation results in the mean spacing of

$a_2= ((a_1/2 + a_1)/2 = 0.75\ a_1$

The behavior with increasing moment M is as follows:

Bending moment	M	increasing
Transition length	a_2	constant
Steel stress	σ	increasing
Crack width	w	increasing
Crack number	n_{cr}	constant

2.1.4 NATURE OF THE CDT

In this sense, there is a continuous transformation from the first into the final crack formation. The Continuous Deformation Theory (CDT) takes its name from this phenomenon. The process can be described thoroughly by knowledge of the phenomena, which occur within the transition length a1. This value obeys the material properties tensile strength of concrete and bond law defining the bond behavior between steel and concrete.

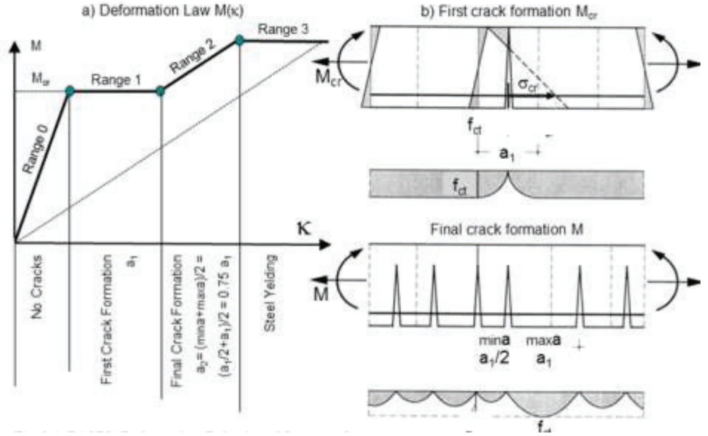

Fig. 2.1:BASES, Deformation Behavior of Concrete Structures

Crack formation and transformation of the transition length a1 into the final crack spacing a_2

a) Deformation Law M(κ), b) First Crack Formation M_{cr}

2.2 LINKS WITHIN THE TRANSITIONS LENGTH FIG. 2.2 [7,15,16, 22, 28, 31]

2.2.1 Crucial Values

The following crucial values within the transition area increase continuously with the distance from the resting point:

Bond stress τ
Steel strain ε
Steel slip δ

2.2.2 LINKS

The crucial values are linked with the following relationships:

- The bond stresses τ are linked with the steel strain by the equilibrium $\Sigma\tau\ C_s = \sigma\ A_s$
- The steel strain ε is linked with the steel displacement by compatibility $\Sigma\varepsilon = \delta$
- The steel displacement is linked with the bond stress τ by the bond law $\tau = A\ \delta^N$

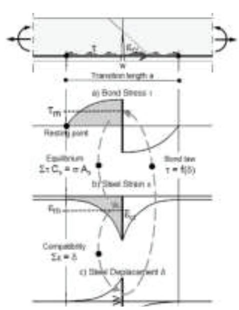

Fig. 2.2: METHOD, Links within the transition length a

a) Bond stress □, b) Steel strain □, c) Steel slip

2.3 MATERIAL BEHAVIOR, FIGURE 2.3, [16]

2.3.1 CRUCIAL MATERIAL PROPERTIES

The occurences regarding cracks obey two material properties – tensile strength of concrete and bond behavior.

2.3.2 TENSILE STRENGTH f_{ct}

The tensile strength of concrete depends on the following four impacts:

- Concrete quality defined by its strength fc
- Pre-damage caused by the own stresses being determined by thickness h
- Related eccentricity η = M/(N h)
- Thickness of the component h

2.3.3 BOND LAW $\tau = f(\delta)$

The bond law depends on the following four impacts:

- Concrete quality defined by its strength fc
- Bond class – top location I or bottom location II within the component
- Related rib area aR defining the bar resistance against displacement
- Related concrete cover c/ds defining its resistance against formation of longitudinal cracks

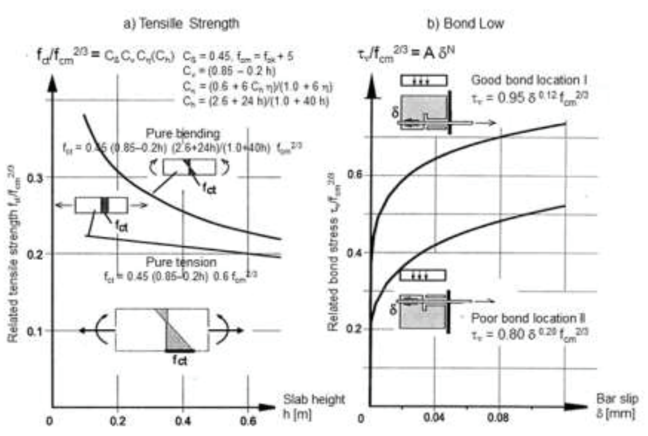

Fig. 2.3: BASES, Crucial material features

a) Tensile strength of concrete fct, b) Bond low □v(d)

3. METHOD

3.1 BASIC CRACK WIDTH EQUATION, FIG. 3.1, [7,15,16, 22, 28, 31]

3.1.1 GENERAL EQUATION FOR w

Crack width w is nothing more than the integral of the steel strains ε_m (σ) within the transfer length a(σ) in which the steel bar is being displaced. Consequently, the crack width can be expressed as follows:

$w = a\ \varepsilon_m$

a transition length needed to induce steel stress into concrete

ε_m mean steel strain within the transition length

So the values a(σ) and $\varepsilon_m(\sigma)$ are needed to determine the crack width. Since both values are functions of steel stress σ, it is obvious that the crack width w depends on σ^2. Realizing that σ depends on M, N and ρ, both these magnitudes must be determined properly to control the crack width effectively. So, the accuracy of the crack width prediction depends primarily on the internal forces M and N. Knowing this, these values must be determined non-linearly by considering their redistribution caused by cracking.

3.1.2 GENERAL EQUATION FOR a

The transition length a is the section of the reinforcing bar at the crack in which the steel moves against concrete. Within this section the high steel stress at the crack is transferred into concrete by bond stresses. The transition length obeys the following equation gained from the equilibrium of the bar section in which bond stress is activated:

$$\Sigma\tau = \Sigma\sigma \Rightarrow 2\ \tau_m\ \pi\ d_s\ a_1 = \pi\ d_s^2/4\ \sigma_{cr} \Rightarrow {}_1 = 0.5\ d_s\ \sigma_{cr}/\tau_m$$

The mean bond stress τ_m is needed to determine the transition length a.

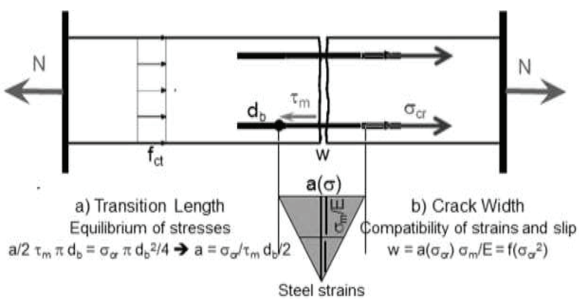

Fig. 3.1: METHOD, Basic crack width equation, a) Transition length a, b) Crack width w

3.2 BOND EQUATION, FIG. 3.2. [7, 15, 16, 22, 28, 31]

3.2.1 DERIVATION

By equating the displacements gained by double integration of τ and by the bond low $\tau = f(\delta)$, the following bond equation is derived:

$[\tau(y)/(A\, f_{cm}^{2/3})]^{1/N} = 4/(d_s\, E_s) \iint \tau(y)\, dy\, dy$, see Fig. 3.2

3.2.2 MEAN BOND STRESS

The bond equation provides the following two crucial magnitudes:

Mean bond stress within the transition area

$\tau_m = [2^{-3N}\, (1\text{-}N)^{(1+N)}/(1+N)\, A/E_s^N\, f_{cm}^{0.66}\, d_s^N\, \sigma_{cr}^{2N}]^{1/(1+N)}$, see Fig. 3.2

The expressions can be simplified by insertion of the bond law values A = 0.95 and N = 0.12:

$\tau_m = (0.13\, f_{cm}^{0.66}\, d_s^{0.12}\, \sigma_{cr}^{0.24})^{0.89}$

3.2.3 MEAN STEEL STRAIN

Mean steel strain within the transition area: $\varepsilon_m = (1\text{-}N)/2\, \varepsilon_{cr}$, see Fig. 3.2

The expressions can be simplified by insertion of the bond law exponent $N = 0.12$: $\varepsilon_m = 0.44\, \varepsilon_{cr}$

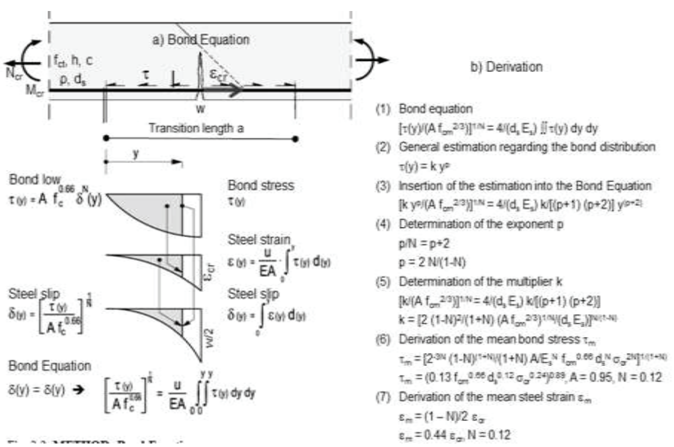

Fig. 3.2: METHOD, Bond Equation

Derivation of the bond stress distribution within the transition area a and mean bond stress t_m, *a) Bond Equation, b) Derivation of* τ_m *and* ε_m

3.3 CRACK WIDTH EQUATIONS, FIG. 3.3, [7, 15, 16, 22, 28, 31]

3.3.1 DESIGN EQUATION

By use of the above input values and by introduction of the crack development factor C_E the following crack equation was found:

$w_k = \gamma_w \cdot C_E \cdot a_1 (\sigma_s - C_E \cdot 0.56 \cdot \sigma_{cr})/E_s$, see Fig. 3.3

3.3.2 METHOD EFFICIENCY

The method covers the following 15 impacts:

Tensile strength f_{ct}	Concrete strength f_{cm}, pre-damage, eccentricity, thickness
Bond law τ	Concrete strength f_{cm}, bar surface a_R, bonding position, concrete cover c/d_s
Actions	Internal forces M and N, temperature
Reinforcement	Ratio ρ, bar diameter d_s
Crack range	First and final crack formation

The continuous crack equation can be adapted for any sort of concrete and steel and for any load actions.

Because of this, the method is generally used in research and in practice.

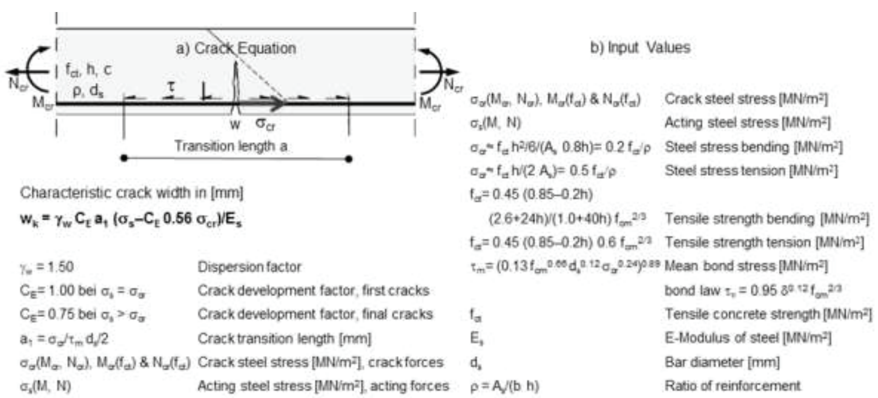

Fig. 3.3: METHOD, Crack Width Equations

Crack prediction method gained from the Continuous Deformation Theory

a) Crack Equation, b) Input Values

3.4 SIMPLIFIED CRACK WIDTH EQUATION, FIG. 3.4, [1, 2, 3, 7, 10, 13, 21]

3.4.1 GENERAL DESIGN EQUATION IN EN 13084 AND CICIND MODEL CODE

Out of the above full crack equation the following simplified equation was derived:

$w_k = 3.5\ (\sigma_{cr}^{0.88}/f_{cm}^{0.66}\ d_s)^{0.89}\ (\sigma_s - 0.4\ \sigma_{cr})/E_s$, see Fig. 3.3 and 3.4

3.4.2 FIRST CRACK FORMATION

In case of the most common first crack formation (acting stress σ_s equals crack stress σ_{cr}) the equation becomes more transparent:

$w_k = 2.1\ (\sigma_{cr}^{2.00}/f_{cm}^{0.66}\ d_s)^{0.89}/E_s$, see Fig. 3.3 and 3.4

3.4.3 DESIGN PROCESS, FIG. 3.4, [7, 15, 16, 22, 28, 31]

The process of the crack control involves the following data collectives:

Input Data Steel and concrete properties, dimensions, loads, temperature

Design Criteria Steel stress $\sigma_s < f_y$, crack width $w_k <$ maxw, bar spacing mins < s < maxs

Output Data Thickness h, ratios of reinforcement ρ, bar diameters d_s

Since such process is not very transparent and requires some effort, appropriate Design Charts are offered in the Design Manual [26].

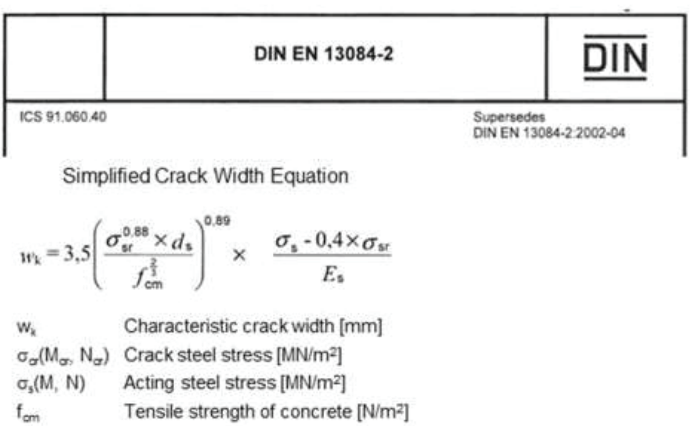
DIN EN 13084-2
DIN
ICS 91.060.40
Supersedes DIN EN 13084-2:2002-04

Simplified Crack Width Equation

$$w_k = 3{,}5\left(\frac{\sigma_{sr}^{0.88} \times d_s}{f_{cm}^{\frac{2}{3}}}\right)^{0.89} \times \frac{\sigma_s - 0{,}4 \times \sigma_{sr}}{E_s}$$

w_k Characteristic crack width [mm]

$\sigma_{cr}(M_{cr}, N_{cr})$ Crack steel stress [MN/m²]

$\sigma_s(M, N)$ Acting steel stress [MN/m²]

f_{cm} Tensile strength of concrete [N/m²]

Fig. 3.4: METHOD, Simplified Crack Width in EN 13084, CICIND Model Code, DIN 1056
Crack prediction method gained from the Continuous Deformation Theory

4. RELIABILITY

4.1 MEASUREMENTS VS. PREDICITIONS, FIG. 4.1, [16, 22]

The aim of the laboratory tests on beams was to gain information about the general crack behavior. The corresponding crack widths w_k were calculated by use of the method in EN 13084. The comparison between the measured and the calculated crack widths confirms the following:

- good agreement between the measured and computed values
- small scatter of only 15% around the ideal line

4.2 IMPACT OF CONCRETE COVER, FIG. 4.2, [16]

The aim of the computation study regarding cracks in beams was to gain clues about the following issues:

- Impact of the features f_c, h, c, ρ and d_s on the behavioral features steel stress σ_s and crack width w
- Comparison of the computation results predicted by EN13084 [03] and by EC 2 [04]

The results of the study regarding the impact of the concrete cover c allow the following statements regarding the agreement between EN 13084 and EC2:

σ_s – Generally good agreement

w_k – Poor agreement in the range c < 30 mm where EC2 behaves incomprehensibly discontinuous

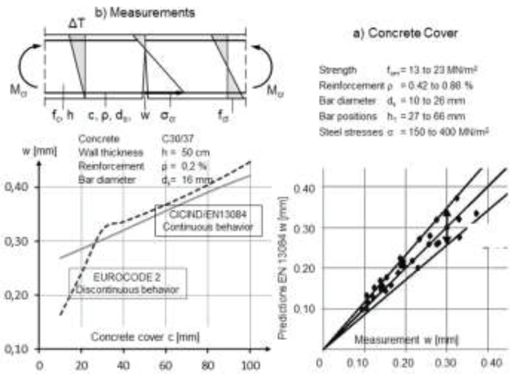

Fig. 4.1: RELIABILITY, Plausibility of the predictions

a) Impact of concrete cover in CICIND/EN13084 and EC 2,

b) Check of the predictions acc. to EN13084

5. APPLIANCE

5.1 PARKING LOT BOTTOM SLAB [27]

5.1.2 SLAB FEATURES, FIG. 5.1.1

Numerous extreme wide cracks with water spills appeared alongside the border of a large foundation slab. The damage was caused by a severe slab cooling in the wintertime which activated tension and produced separating cracks

Fig. 5.1.1: APPLIANCE, Bottom Slab in an Underground Parking Lot
Loss of tightness due to wide through cracks
a) Entrance ramp, b) Wide through cracks with leaking ground water

5.1.2 CRACK FORMATION

The mechanism of the crack formation was as follows:

Temperature drop in wintertime	→ Contraction of the slab
Contraction of the slab	→ Constraint of slab contraction by columns
Constraint of slab contraction	→ Activation of tension forces
Activation of tension forces	→ Formation of individual cracks

5.1.3 CRACK BEHAVIOUR, FIG. 5.1.2

The crack behavior identified by measurements, drilling cores and microscopic photos are as follows:

Numerous individual cracks → increasing number after each sudden frost

Cracks crossing aggregate → formation after the concrete hardening

Wide through cracks 0.8 mm → not tight slab and intrusion of the ground water under pressure

Much wider cracks in coating → delamination and erosion at the crack edges

The leakage was caused by excessive crack widths which enabled the pressurized ground water to intrude into the building. The wide cracks were caused by insufficient reinforcement at the slab top.

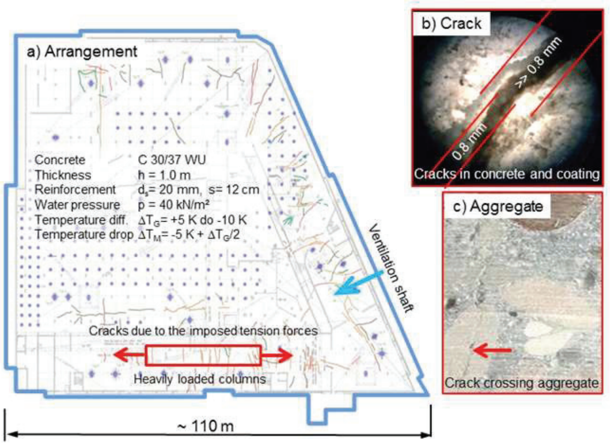

Fig. 5.1.2: APPLIANCE, Bottom Slab in an Underground Parking Lot

a) Crack locations, b) Crack in concrete and coating, c) Crack crossing aggregate

5.1.4 POOR CRACK PREDICTION BY EC2, FIG. 5.1.3

Primarily due to the underestimation of the tensile strength the crack width prediction by EC2 couldn't explain the leakage:

- Assumption of the crack formation at early concrete age with a low tensile strength f_{ct} = 1.5 MN/m^2

- Further reduction of by factor 0.5 through postulation of own stresses f_{ct} = 1.5/2 = 0.75 MN/m^2

- Underestimation of the cracking stress in the reinforcement σ_s = 144 MN/m^2

- Severe underestimation of the crack width w_k = 0.20 mm, which does not explain the water intrusion

5.1.5 CORRECT CRACK PREDICTION BY EN 13084, FIG. 5.1.3

Due to the correct tensile strength the crack width prediction by EN 13084 could explain the wide cracks and the leakage:

- Assumption of the crack formation at mature concrete age with a high tensile strength f_{ct} = 2.1 MN/m^2
- No reduction of the tensile strength by own stresses
- Correct estimation of the cracking stress in the reinforcement σ_s = 404 MN/m^2
- Correct prediction of the crack width w_k = 0.78 mm, which does explain the water intrusion

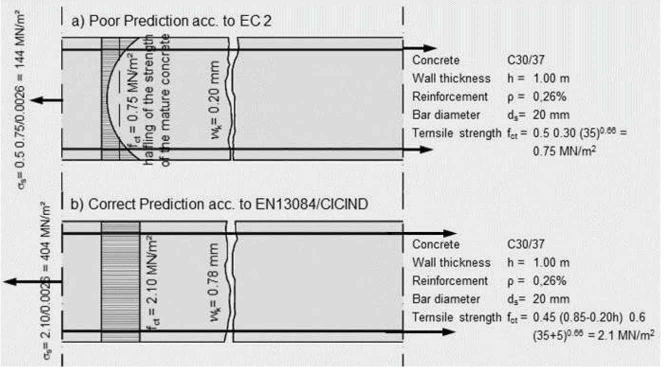

Fig. 5.1.3: APPLIANCE, Bottom Slab in an Underground Parking Lot
a) Poor crack prediction acc. to EC2, b) Correct crack prediction acc. to EN 13084/CICIND

5.2 CHIMNEY WINDSHIELD [16, 22, 25]

5.2.1 WINDSHIELD FEATURES, FIG. 5.2.1

Hoop reinforcement in a new chimney should be designed in terms of the formation of vertical cracks. Such cracks are produced by temperature difference of ΔT > 10K which may easily occur due to sun radiation or sudden frost. These cracks are not a problem if the following values are properly limited:

..steel stress σ_s< 400 MN/m^2 < f_y to prevent formation of dangerous separating through cracks

..crack width w_k < 0.40 mm to prevent severe ruptures of the protection panting which are caching dirt

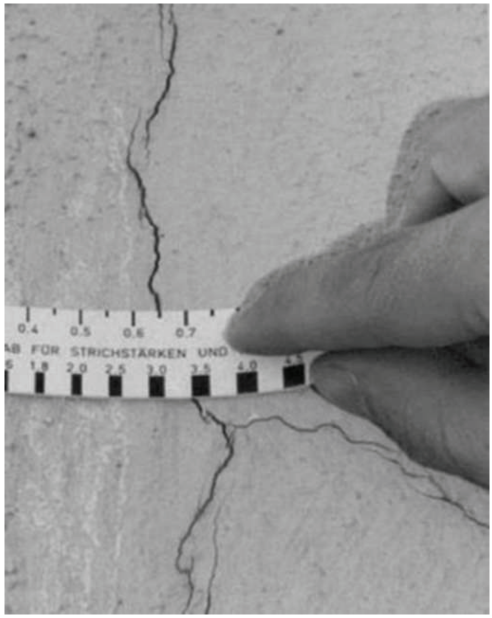

5.2.2 CRACK FORMATION, FIG. 5.2.2

The crack formation can be explained by use of the portion of a windshield section:

Temperature drop in wintertime → Contraction of the external face

Contraction of the external face → Rotation of the considered windshield portion

Rotation of the portion → Initiation of a moment rotating backward

Initiation of a moment → Activation of tension stress at the colder, external windshield face

Activation of tension stress → Formation of cracks at the locations of low tensile strength

Formation of a cracks → Excitation of steel stress/crack width depending on the amount of ρ

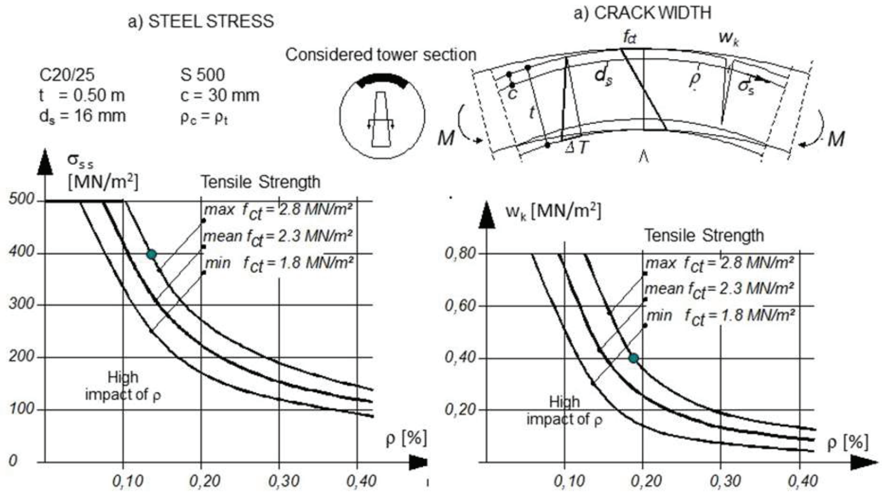

Fig. 5.2.2: APPLIANCE, Windshield of a PP chimney , Impact of reinforcement ρ and tensile strength f_{ct}

a) Steel Stress $\sigma_{s,}$ b) Crack width w

5.2.3 CRACK CONTROL

The process of the crack control involves the following data collectives:

Input Data Steel and concrete properties, dimensions, loads, temperature

Design Criteria Steel stress $\sigma_s < f_y$, crack width $w_k <$ maxw, bar spacing mins < s < maxs

Output Data Windshield thickness h, ratios of reinforcement ρ, bar diameters d_s

REQUIRED REINFORCEMENT, FIG. 5.2.2

The study shows the significance of the amount of hoop reinforcement ρ in case of the maximum tensile strength of concrete f_{ct}:

- Steel stress limitation $\sigma_s < 400$ MN/m^2 requires ρ > 014%
- Crack width limitation $w_k < 0.4$ mm requires ρ > 019%

Despite the minimum hoop reinforcement in standards of 0.2% there are cases in which the crack width must be limited more strictly and so more reinforcement is needed. Interestingly, the values σ_s and w_k react sensitively to reinforcement only below the mark of ρ = 0.40%. So, since the industrial structures are always lowly reinforced their design must occur especially carefully [16, 17].

6. RATINGS

6.1 CRACK SIGNIFICANCE

The considerations in this paper were accompanied by the awareness of the following issues regarding the crack significance:

- Thread by damaging cracks can only occur in lowly reinforced components.
- Crack pattern are mostly characterized by individual cracks located far from each other.
- Formation of cracks is a favorable phenomenon causing a reduction of moments in the cracked areas.
- Reliable methods for crack prediction must satisfy the conditions equilibrium, compatibility bond law.
- Predictions of crack width must be fed with forces gained by use of decreased stiffness due to cracking.

6.2 CLOSENESS TO REALITY

The closeness to reality of the crack width prediction methods presented in this paper are based on its following features:

(1) Consistency with the Continuous Deformation Theory, CDT
(2) Satisfaction of the rules of equilibrium, compatibility and material laws
(3) Applicability to any tensile strength values and bond laws
(4) Validity for any ranges of crack formation
(5) Acceptance of any sorts of actions and eccentricities
(6) Accessibility for all sorts of input values such as
(7) Suitability for stochastically oriented analyses

6.3 ADVANTAGES OF THE METHOD

Due to the above, the crack prediction methods deserve the following ratings:

Physical Purity	Fulfillment of all mechanical rules including the non-linear structure behavior
Simplicity in Use	Presence of one transparent equation for all designing scenarios
Universality in Use	Validity for all crack formation ranges, any reinforcement, any eccentricities
Closeness to Reality	Agreement with test results and experiences
Wide Acceptance	Entry into several standards and general use in research and practice

All in all, the crack prediction methods have been accepted in the international standards EN 13084 and CICIND. So, the methods are worldwide in use for advanced design of such industrial structures as chimneys, containments, cooling towers, industrial floorings, storage tanks, etc. Since in such sort of structures tightness is the most important design criterion, the prediction of crack width must occur by use of this reliable method.

REFERENCES

1. Bergmeister, K.: Risse im Konstruktionsbeton. Beton- und Stahlbetonbau 94 (1999), H. 6, S. 245-253
2. CICIND: Model Code and Commentaries for Concrete Chimneys. Part A: The Shell CICIND 1984 & 2008,
3. EN 13084: Freistehende Schornsteine, Teil 2: Betonschornsteine. Normenausschuss Bauwesen (NABau) im DIN e.V., April 2007
4. EUROCODE 2: Design of concrete structures CEN, European Committee For Standardization 2004
5. Harling A., Noakowski P., Rost M.: The Crack Width Prediction in EN 13084 – Background, Method, Reliability, Appliance, Appraisal. CICIND-Report, 2014
6. Harling, A.: Maste und Türme aus hochfestem Beton, Wirklichkeitsnahe Erfassung der Rissbildung zylindrischer Baukörper, Technische Universität Dortmund, Schriftenreihe Betonbau, Heft 7, 2015
7. Harling, A., Noakowski, P., Maurer, R.: Erfassung der Rissbildung in Masten und Türme aus hochfestem Beton, Ernst & Sohn Fachmagazin Beton- und Stahlbetonbau 4/2016
8. Knauf, M., Grzeszykowski, B., Golubinska, A.: Minimum Reinforcement for Crack Width Control in RC Tensile Elements. DO1: 10.2478/ace 2019-008
9. Lohmayer, G.: Weiße Wannen, einfach und sicher. Verlag Bau + Technik 2009
10. Moncarz, P., Noakowski, P., Ross, B.: Constraint Cracking in Continuous Pier Supported Beams. 1st Conference on Concrete & Structures, Kuala Lumpur 1989.
11. Moncarz, P., Noakowski, P.: Analysis of long-term Performance of Prestressed Concrete Pipes. XI FIP Congress, Hamburg 1990.
12. Nieser, H., Engel, V.: Industrieschornsteine in Massivbauart. Kommentar zu DIN 1056, 1986.
13. Noakowski, P., Baumann, T., Topp, T., Aigner, F.: Vorgespannte Flüssiggas-Behälter. Bauinformatik (1991), H. 6.
14. Noakowski, P., Keuser, M., Brunssen, G., Günther, H.: Stahlbetontunnel. Bauinformatik (1992), H. 3.
15. Noakowski, P., Moncarz, P.: Stiffness Oriented Design of R. C. Structures. Księga Jubileuszowa Profesora Tadeusza Godyckiego-Ćwirko, Politechnika Gdańska, Gdańsk 1998
16. Noakowski, P., Schäfer, H.G.: Steifigkeitsorientierte Statik im Stahlbetonbau. Buch, Ernst & Sohn, 2003
17. Noakowski, P., Breddermann, M., Harling, A., Schnetgöke, J.: Rissbildung in turmartigen Tragwerken, Mast vs. Schornstein, Beton- und Stahlbetonbau 100 (2005), H. 7, S. 538-548
18. Noakowski, P., Breddermann, M., Harling, A., Rost, M.: Turmartige Industriebauwerke, Grundlagen der CICIND, DIN EN 13084, Betonkalender 2006, Ernst und Sohn
19. Noakowski, P., Leszinski, H., Breddermann, M., Rost, M.: Schlanke Hochbaudecken, Beton- und Stahlbetonbau 103 (2008), H. 1, S. 28-37
20. Noakowski, P., Harling, A., Breddermann, M., Rost, M.: Windkraftanlagen… Die Bautechnik, September 2009, Ernst und Sohn
21. Noakowski, P., Breddermann, M., Harling, A., Rost, M., Potratz, S., Leszinski, H.: Verstärkung turmartiger Bauwerke, Sonderheft „Kraftwerksbau“, Ernst & Sohn, Dezember 2009
22. Noakowski, P.: Close to reality methods for the structural design of towers. Architecture, Civil Eng., Environment, The Silesian Univ. of Technology, Vol. 3/2010
23. Noakowski, P., Breddermann, M., Harling, A., Rost: Cracks in Windshield Caused by Foundation Settlements ISCT, 6th International Symposium on Cooling Towers, Köln 2012

24. Noakowski, P., Harling, A.: Strengthening of the TV-Tower Düsseldorf by a near-surface reinforcement of FRP, 1st CECOM, Lodz University of Technology, Krakow 2012
25. Noakowski, P.: Proper design of the r/c structures in terms of use of the realistic moments CCC 2013, Central European Congress on Concrete Engineering, Wroclaw, September 2013
26. Noakowski, P., M., Harling, A., Rost, M.: Manual for the Design of Concrete Chimneys CICIND Autumn Meeting, Paris, October 2013
27. Noakowski, P., M., Harling, A., Michalak, B.: Szczelność płyty fundamentowej pod maszynownię ENERGIA 2014, Karpacz Polen, Mai 2014
28. Noakowski, P., M., Harling, A., Zdanowicz, L.: About the crack width prediction AMCM 2014, 8th International Conference, Wroclaw 2014
29. Noakowski, P.: Safe and economic design of r/c structures by use of proper bending moments. Politechnika Krakowska, Conference "Practical applications of innovative solutions", Krakow 2015
30. Noakowski, P., Moncarz, P., Harling, A.: The crack width prediction in EN 13084, application for LNG aci, The Concrete Convention, Denver October 2015
31. Noakowski, P., Harling, A.: The crack width prediction in EN 13084, application for chimneys 87th CICIND Conference, Singapore Mai 2017
32. Pfefferkorn, W., Steinhilber, H.: Ausgedehnte fugenlose Stahlbetonbauten. Beton-Verlag 1990
33. Rüsch, H., Rehm, G.: Versuche mit Betonformstählen, Deutscher Ausschuss für Stahlbeton, Hefte 140 und 160, Beuth Verlag
34. Schnell, J., Kautsch, R., Noakowski: Verhalten von Hochbaudecken bei Zugkräften aus Zwang. Beton- und Stahlbetonbau 100 (2005), H. 5, S. 406-415
35. VGB PowerTech: Industrieschornsteine, Hinweise zur Bauausführung und Inbetriebnahme Merkblatt, VGB-M 642 U, Essen 2019
36. Walraven, J. C., Shkoukani, H.: Kriechen und Relaxation des Betons bei Temperaturzwangbeanspruchung, Beton- und Stahlbetonbau 88 (1993), Heft 1, S. 10 – 15.
37. Zilch, K., Niedermeier, R., Finckh, Wolfgang: Strengthening of Concrete Structures with Adhesively Bonded Reinforcement, Wiley Ernt & Sohn,

LIST OF FIGURES AND TABLES:

Fig. 1.1: BACKGROUND, Threats by wide separating cracks

Loss of the wind load bearing capacity due to wide separating cracks

a) Normal cracks due to enough hoop reinforcement, Regular vertical stresses

b) Separating cracks due to insufficient hoop reinforcement, Increased vertical stresses

Fig. 1.2: BACKGROUND, Impairments by Wide Cracks

a) Impairment of the visibility of industrial chimneys by depositions of dirt into wide cracks in painting

b) Destruction of the integrity of industrial chimneys by water intrusion into wide cracks and ice formation

c) Endangering of the wind bearing capacity of cooling towers by shell separation into free-standing walls

Fig. 2.1: BASES, Deformation Behavior of Concrete Structures

Crack formation and transformation of the transition length a_1 into the final crack spacing a_2

a) Deformation Law M(κ), b) First Crack Formation M_{cr}

Fig. 2.2: METHOD, Links within the transition length a

a) Bond stress τ, b) Steel strain ε, c) Steel slip δ

Fig. 2.3: BASES, Crucial material features

a) Tensile strength of concrete f_{tc}, b) Bond low $\tau_v(d)$

Fig. 3.1: METHOD, Basic crack width equation

a) Transition length a, b) Crack width w

Fig. 3.2: METHOD, Bond Equation

Derivation of the bond stress distribution within the transition area a and mean bond stress t_m

a) Bond Equation, b) Derivation of τ_m and ε_m

Fig. 3.3: METHOD, Crack Width Equations

Crack prediction method gained from the Continuous Deformation Theory

a) Crack Equation, b) Input Values

Fig. 3.4: METHOD, Simplified Crack Width in EN 13084, CICIND Model Code, DIN 1056

Crack prediction method gained from the Continuous Deformation Theory

Fig. 4.1: RELIABILITY, Plausibility of the predictions

a) Impact of concrete cover in CICIND/EN13084 and EC 2, b) Check of the predictions acc. to EN13084

Fig. 5.1.1: APPLIANCE, Bottom Slab in an Underground Parking Lot

Loss of tightness due to wide through cracks

a) Entrance ramp, b) Wide through cracks with leaking ground water

Fig. 5.1.2: APPLIANCE, Bottom Slab in an Underground Parking Lot

a) Crack locations, b) Crack in concrete and coating, c) Crack crossing aggregate

Fig. 5.1.3: APPLIANCE, Bottom Slab in an Underground Parking Lot

a) Poor crack prediction acc. to EC2, b) Correct crack prediction acc. to EN 13084/CICIND

Fig. 5.2.1: APPLIANCE, Windshield of a PP chimney

a) Chimney of 150 m height in Berlin, b) Wide crack 0.65 mm due to insufficient hoop reinforcement

Fig. 5.2.2: APPLIANCE, Windshield of a PP chimney

Impact of reinforcement ρ and tensile strength f_{ct}

a) Steel Stress $\sigma_{s,}$ b) Crack width w

Received 18.04.2019 , Revised 20.02.2020